Check for updates

Underwater Cultural heritage risk assessment methodology for wave-induced hazards: The showcase of the Bay of Cadiz

Tomás Fernández-Montblanc[1]*, Manuel Bethencourt[2] and Alfredo Izquierdo[3]

[1]Earth Sciences Department, University of Cadiz INMAR, Puerto Real, Spain, [2]Department of Materials Science, Metallurgy Engineering and Inorganic Chemistry, University of Cadiz INMAR, Puerto Real, Spain, [3]Applied Physics Department, University of Cadiz INMAR, Puerto Real, Spain

Coastal areas are characterized by high energetic conditions associated to the wave transformation process and by numerous underwater cultural heritage (UCH) sites whose preservation is crucial given their cultural and economic value. UCH management requires a decision support system to prioritize UCH interventions and actions for long-term preservation. This paper presents a novel UCH risk assessment methodology to quantitatively assess the impact of wave-induced hazards on UCH in coastal environments at a local level and the screening of UCH sites at risk. The UCH risk is calculated as a function of vulnerability (depending on archaeological materials, slope, and seabed type), hazard (decontextualization, scouring, and erosive wear), and exposure computed for the UCH sites registered in an archaeological database. The procedure was validated at two shipwreck sites, *Bucentaure* and *Fougueux*, in the Bay of Cadiz. An agreement between the risk index value and the *in situ* measurements of the rates of scouring and corrosion (used as a proxy of erosive wear) was observed. The methodology was tested in the Bay of Cadiz using an archaeological database containing 56 UCH sites. It allowed identifying the UCH sites at high risk: six are at risk of decontextualization, four are in peril of scouring erosion, and two are at risk of erosive wear. Two UCH sites at high risk of at least two hazards were also identified. This UCH risk assessment methodology is a stepping stone towards a decision support system that will give priority to research, prospection, management, and protection measures in the UCH sites analyzed to ensure their preservation in a context of climate change in the era of a sustainable blue economy.

1 Introduction

A large number of underwater cultural heritage (UCH) sites are characteristic of coastal areas as a result of the intense use of those areas for human settlement as well as commercial and military purposes for centuries. The concentration of UCH sites is also a direct consequence of coastal sailing and perils such as stormy weather conditions, rocky shoals, or other hazards existing in those areas used for coastal navigation. Shallow coastal waters therefore contain numerous UCH sites. Intensive exploitation of ocean resources, along with the advances in acoustic seafloor mapping, and the expansion of scuba diving in recent decades have contributed to their discovery. Considering the abundance of shipwreck sites and other underwater archaeological structures, an archaeological study or *in situ* protection of all of them is currently unaffordable. Adopting measures to protect underwater archaeological remains, in accordance with the Convention on the Protection of the Underwater Cultural Heritage United Nations Educational, Scientific and Cultural Organization (UNESCO), is challenging when a large number of sites should be managed and considered for interventions with a limited budget.

Furthermore, shallow coastal waters are a very energetic environment where oceanographic agents such as waves, currents, and sediment characteristics determine a dynamic equilibrium. Changes in energetic (*e.g.*, seasonal) conditions can generate the successive burial and exposure of UCH sites (Gregory et al., 2012; Fernández-Montblanc et al., 2016; Fernández-Montblanc et al., 2018), affecting the stability and degradation of UCH materials (Bethencourt et al., 2018; Gregory, 2020). These agents can control the proliferation of harmful organisms for the materials (Ruuskanen et al., 2015; Cámara et al., 2017; González-Duarte et al., 2018), sediment transport, and elimination of concretion layers that act as protective covers of certain archaeological objects (Bethencourt et al., 2018). Therefore, the degradation of UCH sites (Pournou, 2018; Gregory, 2020) may be aggravated in shallow water areas. At the UCH sites located in coastal waters, the degradation rates may experience episodic fluctuations associated with changes in the energetic conditions in the system (Ward et al., 1999). Waves can be considered a major hazard driver for the conservation of UCH sites in wave-exposed coasts. Given the magnitude of the wave force exerted and the sediment transport capacity in shallow water depths, waves contribute to the scattering of archaeological objects and induce scouring or abrasion by displacing sand grains. This results in the loss and degradation of archaeological material.

The scattering of archaeological objects or shipwreck remains caused by waves leads to archaeological decontextualization. It occurs when archaeological objects are transported from their original wreckage location, losing connectivity with their original context and other related archaeological objects.

Decontextualization of UCH artefacts occurs when drag forces induced by waves on the seabed are large enough to transport objects located at the UCH site. Additionally, wave forces and wave load can damage and transport part of the structure of a shipwreck, producing the disintegration and decay of the archaeological structure.

Wave-induced oscillatory flow and turbulence may lead to scouring around the shipwreck or other UCH sites (Quinn, 2006; Fernández-Montblanc et al., 2016). Scouring is a key process for the conservation of UCH because it is able to control the sediment budget around UCH sites. It is the result of the intensification of flow velocity by its interaction with near-seabed objects (Whitehouse, 1998). Scouring largely controls the integrity of the UCH sites. A wooden hull structure can collapse if a scour pit is formed around the archaeological remains. It determines the exposure of the archaeological material to the abrasive effect caused by the suspended sediment particles and also produces drastic changes in other environmental variables (*i.e.*, oxygen concentration, benthic communities) governing the deterioration process (Ward et al., 1999; Quinn, 2006; Bethencourt et al., 2018; Gregory, 2020), for example, scour can increase the oxygen concentration that accelerates the microbial degradation process of the wooden remains (Björdal et al., 2000; Björdal and Nilsson, 2008) and increase the corrosion rates of active metals such as copper or iron (Angelini et al., 2013). Scour also controls the composition of the benthic community that affects the conservation of metallic objects (Bethencourt et al., 2018) or the degradation of stone materials (Cámara et al., 2017). The amplification of maximum orbital velocity and the appearance of shear stress and coherent flow structures caused by waves and seabed structure interactions are the main mechanisms in generating scour associated to waves (Sumer and Fredsøe, 2002). Wave-induced scour will vary depending on the structure's size and wave conditions (McNinch et al., 2006; Fernández-Montblanc et al., 2016).

Suspended sediment transported by currents or waves can produce abrasion by impacting on the surface of the archaeological materials [see Thompson et al. (2011)]. Erosive wear, a wave-induced hazard on UCH, is the process of progressively removing material from a surface due to the repeated impacts of solid particles present in the flow. If there is enough energy, each particle re-suspended in the flow can cut or fracture a small amount of material from the surface. If this is repeated over a long period of time, a significant loss of material may occur. The rate of erosive wear depends on several factors. The characteristics of the suspended particle and its shape, hardness, impact velocity, and impact angle are key factors, along with the properties of the surface being eroded (Bitter, 1963).

Hence, given the profusion of UCH sites in coastal areas and the hazardous conditions linked to wave action, the development of tools and methodologies to select and identify sites prone to

damage is necessary. This is especially relevant in a context of climate change, given the significant changes in wave energy expected by the end of the century (Mentaschi et al., 2017). These methods will allow the screening of UCHs that are more susceptible to be impacted by waves. It provides UCH managers with a tool for decision support in order to prioritize UCH interventions. This tool gives precedence to UCH sites where special measures must be implemented for *in situ* protection or where excavation and documentation must be a priority, as the loss of archaeological information is highly likely.

The present work therefore aims to develop a risk assessment method that takes into account the impact of wave-induced hazards on underwater cultural heritage. This paper is structured as follows: The Methods section describes the methodology developed and the datasets used to validate the proposed methodology; the Results section outlines the main results, including validation and UCH risk assessment in the case of the Bay of Cadiz; in the Discussion section, the applicability, limitations and potential of the methodology are analyzed based on the achieved results; and, finally, the main findings of this paper are summarized.

2 Methods

2.1 Study area

The Bay of Cadiz is an inlet located in the Gulf of Cadiz (southwest coast of the Iberian Peninsula) extending from Punta Candor to Sancti Petri tidal creek (Figure 1A). The seafloor mainly consists of unconsolidated sediments in which the mean grain size varies from very fine quartz sand to very fine gravel. Exceptions in this general pattern are the bedrock crops in the study area (Figure 1A). Wind waves can be considered the key hydrodynamic agent in the area with regard to UCH preservation. The active sector is defined between NNW and SE, with W being the most frequent and WSW the most energetic direction (Figure 1B). Mean wave climate is characterized by low energy [90% of significant wave height (Hs) is<1 m], although Hs can exceed 3 m for 105 hours in an average year (Figure 1C). The peak wave period (Tp) is rarely over 18 s, and the Hs–Tp joint probability plot shows two peaks from 5 to 9 s, and Hs =1 m, which are representative of mean conditions, whereas for storm wave conditions, it is represented by Tp ~8–12 s and Hs > 3 m (Figure 1D). Tides are semi-diurnal, and the tidal range can be defined as meso-tidal (mean spring range of 2.96 m). Tidal current velocity decreases rapidly in shallow water areas with the exception of the channels and tidal creeks in the Bay of Cadiz.

From a historical and archaeological point of view, because of how old the Bay of Cadiz is as a center of sustained port dominance and the dynamism of the region in terms of maritime cultural activity for millennia, an incredibly large number of

UCH sites are observed. Among the existing archaeological sites, two coetaneous shipwrecks were selected to validate the UHC risk assessment methodology: the *Fougueux* and *Bucentaure* shipwreck sites. Both ships sank during a violent storm after the Battle of Trafalgar (1805). The *Bucentaure* represents a scattered shipwreck site including a total of 22 iron guns and the remains of an anchor (Figure 1E) seated at 12-m depth in the outer Bay of Cadiz (Figure 1A). The seafloor is a combination of a rocky seabed and gravelly quartz sand (D50 = 1.095 mm). Meanwhile, the *Fougueux* shipwreck site preserves an important portion of the wooden hull structure along with 31 cannons and an anchor (Figure 1F). *Fougueux* is seated at 7-m depth, and the seabed is mainly composed of unconsolidated sediments, medium and fine quartz sands (D50 = 0.177 mm), and a little rock shoal attached to the hull remains of the shipwreck.
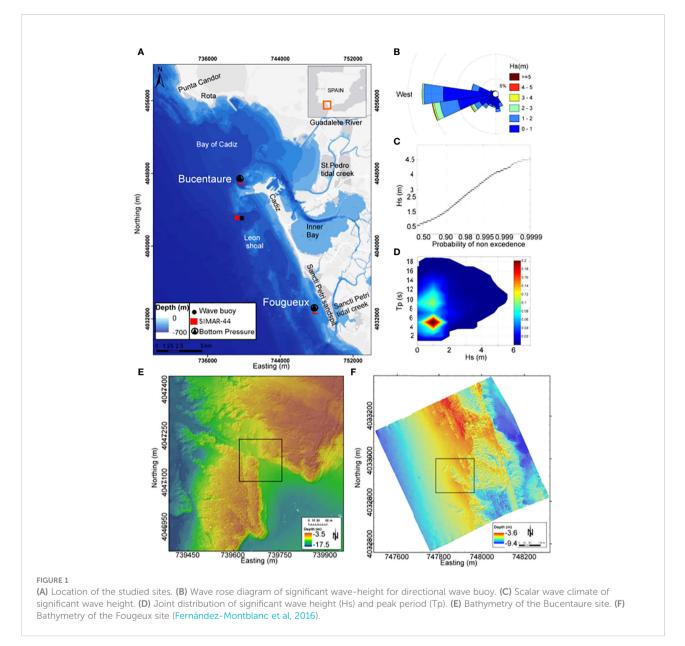
2.2 Environmental and archaeological datasets

2.2.1 Bathymetry and sediment characterization

The present work is based on an eco-cartographic study including bathymetry and sediment characterization performed in 2011 (Spanish Ministry of Agriculture, Food and Environment, 2012). Multibeam-derived bathymetry was used for seafloor characterization in the wave model and to calculate the seabed slope. Seafloor mapping from multibeam backscatter was used to classify the seabed type (rocky/unconsolidated sediment). We used data from a field study in the whole Bay of Cadiz comprising 460 samples collected using a Van Veen grab sampler for sediment grain size characterization. A grain size analysis was conducted using the dry sieving method. The statistics of particle size distributions were calculated using the Folk and Ward method with the GRADISTAT software developed by Blott and Pye (2001).

2.2.2 Archaeological database

We created a dedicated archaeological database (ADB) for the Bay of Cadiz based on a scientific literature review including books, papers, and/or conference proceedings. Several bibliographic sources were employed (Guillemot and Meanteau; Lagostena, 2009; Lakey, 1987; García Rivera and Alonso Villalobos, 2005; Alzaga García et al., 2022). The ADB encompasses the archaeological resources identified and geo-localized in the outer Bay of Cadiz. The geolocation of the different UCH sites was established by georeferencing maps and figures of the scientific data sources in ARCGIS 10.1. The ADB contains relevant information about the main characteristics of the UCH sites including origin or provenance, chronology, composed materials organized into five categories (metallic, stone, glass, ceramic, and wood/organic materials), dominant material, and metadata regarding the data source. Basic

FIGURE 1

(A) Location of the studied sites. (B) Wave rose diagram of significant wave-height for directional wave buoy. (C) Scalar wave climate of significant wave height. (D) Joint distribution of significant wave height (Hs) and peak period (Tp). (E) Bathymetry of the Bucentaure site. (F) Bathymetry of the Fougeux site (Fernández-Montblanc et al, 2016).

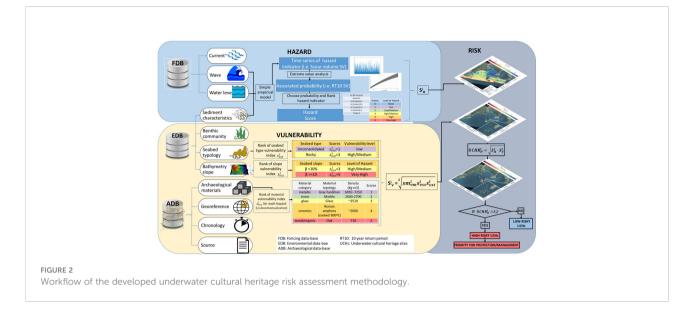environmental characteristics of the sites (depth and seabed type), when available, were also added.

2.2.3 Wave database

A simplified version of the hybrid downscaling method (Camus et al., 2011; Diaz-Hernandez et al., 2021) was used to propagate the historical wave hindcast (SIMAR-44) in the outer Bay of Cadiz (Figure 1A). At first, a manual selection of a reduced number of sea states representative of the offshore wave hindcast climate was performed. Then, the selected N sea-states were propagated into the outer Bay of Cadiz using the SWAN third-generation wave model (Booij et al., 1999) implemented on a regular mesh (~37-m resolution). Finally, the whole wave hindcast in each cell of the computational domain was reconstructed based on the interpolation in a 3D matrix of

propagation coefficients for wave direction, peak period, significant wave height, and maximum near-bottom orbital velocity.

2.3 UCH risk assessment

The present work uses the 2009 UNISDR terminology on disaster risk reduction (https://www.undrr.org/terminology), and risk (R) is calculated as a function of the hazard (H) with a given probability, vulnerability (V), and exposure (E) [R = f(H, V, E)] (Field and Barros, 2014). We developed an UCH risk assessment methodology, whose workflow is schematized in Figure 2. The UCH risk assessment presented here is based on the risk index calculated at each specific location in accordance

FIGURE 2
Workflow of the developed underwater cultural heritage risk assessment methodology.

with the main environmental and UCH site characteristics following an object-oriented approach. Each specific site registered in the archaeological database was considered an asset to be potentially damaged by the considered hazard. This paper focuses on the identification and screening of those UCH sites at high risk, where waves may imperil the sites, thus facilitating the loss of archaeological information and the degradation of archaeological materials and hampering the *in situ* preservation of UCH sites considered as a priority option. This conservation approach is included in Rule 1 of the Guidelines to the Annex of the Convention on the Protection of the Underwater Cultural Heritage—UNESCO that establishes *in situ* preservation as the first option for UCH protection. The methodology followed the scheme used in previous studies on coastal risk assessment at the regional scale [*i.e.*, CRAFT1 (Armaroli and Duo, 2018; Ferreira et al., 2018)]. A GIS index and a simple empirical model-based approach were integrated to support decision making and prioritizing the investment in available resources and actions to counteract the effect of wind waves in the UCH sites at high risk.

The methodology was designed to be applied from the local to the regional scale ≈O (10–100 km), targeting to avoid the request of very detailed environmental information (*e.g.*, DEM resolution<1 m).

A complete risk assessment would require exposure quantification based on the valuation of UCHsites. This high level of baseline information is rarely available at the local or regional scales. Therefore, we considered a similar market and not market value for all the UCH sites in the database, assuming equal exposure values for all the UCH sites. The risk index was then calculated as the root geometric mean of the hazard multiplied by vulnerability scores according to Eq. 1 (Gornitz, 1990; Viavattene et al., 2018).

$$UCHR_H^i = \sqrt{S_H^i \cdot S_V^i} \qquad \text{Eq. 1}$$

where $UCHR_H^i$ is the UCH risk index for each hazard (*H*) at each specific archaeological site (*i*), S_H^i is the score of the hazard, and S_V^i is the score of the vulnerability at site *i*. $UCHR_H^i$ is an index (integer values from 0 to 5) associated to each UCH site that allows quantitatively comparing different UCH sites located in the region of analysis and showing the UCH sites at high risk of the specific hazards. The S_H^i is a six-class score ranging from 0 to 5 which correspond to none, low, low-medium, medium-high, high, and very high hazard. The level of hazard is defined in accordance with the magnitude of the hazard associated to a given non-exceedance probability expressed as a return period. The S_V^i is a score which ranges from 1 to 5 (low to very high classes) that represents the vulnerability of the UCH sites according to the characteristics of the archaeological material prevalent in the UCH site, its propensity to be affected by a certain hazard, and the environmental factors that increase or reduce the susceptibility of the UCH sites to the impacts produced by the considered hazards.

An UCH site is considered at risk if the risk index $UCHR_H^i$ >3.2. This threshold corresponds to the rounded root square of low (2) and very high (5) classes (Viavattene et al., 2018). UCH sites with higher values are those subject to the combination of medium and very high classes of vulnerability and hazard.

The vulnerability and hazard levels at each UCH site are specified in the sections below and summarized in Tables 1, 2. There is a lack of information relative to the definition of the hazard and vulnerability threshold to define the different categories of hazard and vulnerability levels. Therefore, those levels have been defined by expert judgment with local knowledge in oceanography and UCH conservation. The group of experts includes oceanographers, archaeologists, conservators, biologists, physicists, chemists, and engineers.

TABLE 1 Hazard indicator scores for decontextualization, erosive wear, and scouring.

Critical size of decontextualized object, Dcr (m) RT10	Erosive wear potential, EWP (J/m³)RT1	Scouring volume, SV (m³) RT10	Scores	Level of hazard
Dcr< 0.02	-20 ≥ EWP<-18	SV< 0.05	0	None
0.02 ≥ Dcr<0.04	-18 ≥ EWP<-16	0.05 ≥ SV<0.1	1	Low
0.04 ≥ Dcr<0.08	-16 ≥ EWP<-13.5	0.1 ≥ SV<0.15	2	Low/medium
0.08 ≥ Dcr<0.12	-13.5 ≥ EWP<-12.5	0.15 ≥ SV<0.3	3	High/medium
0.12 ≥ Dcr<0.16	-12.5 ≥ EWP<-11.5	0.3 ≥ SV<0.4	4	High
Dcr ≥ 0.16	EWP ≥ -11.5	SV ≥ 0.4	5	Very high

RT10 corresponds to the value of a 10-year return period and RT1 to a 1-year return period.

2.4 Hazard assessment

Previous studies have identified physical factors (Ward et al., 1999) and, more particularly, wind waves to be key in preserving UCH and in the evolution of UCH sites in shallow water sites (Quinn, 2006; Fernández-Montblanc et al., 2016). This work therefore focuses on wave-induced hazards on archaeological sites in shallow water. Three wave-induced hazards were selected considering their impact in the long-term preservation of UCH: archaeological decontextualization), scouring (SC), and erosive wear (EW). For those hazards, risk assessment was performed independently without taking into account multi-hazard interactions.

A simple three-step workflow was applied for the hazard assessment (Ferreira et al., 2018; Viavattene et al., 2018). First, the time series of the hazard indicator was calculated in accordance with bathymetry, sediment, grain size, wave characteristics, and water level. Second, a fit to an extreme value distribution was applied to calculate the associated probability. In this case, the transformed-stationary methodology was applied, including a 72-h time window for storm decluttering and a constant threshold (97th percentile) to select the extreme event. Then, the selected hazard events were fit into the generalized Pareto distribution [see Mentaschi et al. (2016) for further details]. Finally, the hazard scores were defined by ranking the hazard indicator for the selected probabilities.

This methodology followed the so-called response approach (Garrity et al., 2007), which is widely used for coastal storm impact assessment. This approach consists in calculating the probability of occurrence of the hazard (i.e., archaeological decontextualization),

TABLE 2 Vulnerability scores in common materials in underwater cultural heritage sites for decontextualization, erosive wear, and scour hazard.

Material category	Material type	Property: density (kg·cm³)	Property: Brinel hardness scale	Proxy sensitivity to aerobic biological communities	Vulnerability score
Decontextualization					
Metallic	Gray iron	6.95–7.25			1
Stone	Marble	2.6–2.8			2
Glass	Glass	~2.52			3
Ceramics	Coarse ware	~2.0			4
wood/organic	Oak	0.71			5
Erosive wear					
Glass	Glass		482–550		1
Metallic	Gray iron		140–250		2
Ceramics	Coarse ware		120–125		3
Stone	Marble		35		4
Wood/organic	Oak		4–8		5
Scour					
Stone	Marble			–	1
Metallic	Gray iron			–	2
Ceramics	Coarse ware			+	3
Glass	Glass			++	4
Wood/organic	Oak			+++	5

The increase in sensitivity to biologial degradation is indicated from low sensitivity (–) to very high sensitivity (+++).

but not of the driver, or variables governing the hazard (*i.e.*, water level, wave period and significant wave height).

2.4.1 Archaeological decontextualization hazard

The decontextualization of an UCH artefact occurs when drag forces induced by waves on the seabed are sufficient to transport objects located in the UCH site. Furthermore, wave forces and wave load can damage and transport part of the damaged structure away from the shipwreck site, producing the disintegration and decay of the archaeological structure (Ward et al., 1999). The potential damage of scattering and loss of archaeological artifacts induced by waves was evaluated using Eq. 2 as proposed by Soulsby (1997) for the threshold motion of large-diameter particles, taking into account the sole action of wind waves.

$$Dcr = \left(\frac{97.9 U_b^{3.08}}{Tp_{1.08} \left[g \left(\left(\frac{\rho_s}{\rho} \right) - 1 \right) \right]^{2.08}} \right)^{0.5} \qquad \text{Eq. 2}$$

where U_b is the undisturbed near-bed orbital velocity, T_p is the peak wave period, g is the gravitational constant, ρ_s is the density of the grain sediment, and ρ is the seawater density.

The scattering and loss of archaeological objects at UCH sites depends on the material, size, and shape of the archaeological objects. For the sake of simplicity, in the present study, a spherical shape and quartz density (2,600 kg m^{-3}) was assumed based on the shape and density of the material employed to derive the empirical Eq. 2. This assumption does not represent the specific shape and density of the archaeological materials but allows calculating the potential decontextualization comparing the hazard of the different UCH sites without requesting specific and detailed information on the size, shape, or density of the objects or structures in the UCH sites. This information is incorporated into the risk assessment by specifying the vulnerability in accordance with the type of the archaeological material. Table 1 shows the decontextualization hazard scores. In this case, the selected probability corresponds to the 10-year return period, an intermediate value in the extreme distribution. The ranges of the hazard magnitude to score the hazards were defined and compliant with expert judgment based on local knowledge.

2.4.2 Scour hazard

The potential scour was estimated using the equilibrium scour depth. Calculating the equilibrium scour depth was based on Eq. 3 for maximum scour depth and Eq. 4 (Sumer and Fredsøe, 1990) for the maximum scour length for wave-induced scour on pipelines. A constant archaeological object/structure of a cylindrical shape of 1 m in diameter was assumed.

$$S_{max} = D \cdot 0.1 \cdot \sqrt{KC} \qquad \text{Eq. 3}$$

$$L_{Smax} = D \cdot 0.35 \cdot KC^{0.65} \qquad \text{Eq. 4}$$

where $KC = U_b \cdot T_p / D$ is the Keulegan–Carpenter dimensionless number, U_b is the maximum undisturbed near-bed orbital velocity, T_p is the peak wave period, and D is the structure diameter (1 m).

In the of case of breaking or near-breaking wave conditions, the equilibrium scour depth was calculated according to expressions Eq. 5 and Eq. 6 proposed by Young and Testik (2009) for vertical and semicircular breakwaters applied for conditions $0.6 < KC_H = \leq 9.0$ *and* $0.4 < fb = \leq 1.7$,

where KC_H is the Keulegan–Carpenter number expressed as a function of the significant wave height (H_s, $KC_H = H_s \cdot \pi / D$), and fb is the ratio of the water depth and structure height $(h - D)/H^s$, h is the water depth, and D is the structure/object diameter:

$$S_{max} = D \cdot 0.125 \cdot KC_H \sqrt{\psi} \qquad \text{Eq. 5}$$

$$L_{Smax} = \begin{cases} D/2 \cdot KC_H, & KC > \pi, \ detached \ scour \\ D \cdot KC, & KC_H \leq \pi \ attached \ scour \end{cases} \qquad \text{Eq. 6}$$

Both equations allow calculating the maximum scour depth and the length of the scour hole. If the scour mark is approximated to a triangular shape, the volume of scour can be calculated (Eq. 7) and used as an indicator of the magnitude of the scour.

$$SCV = \frac{1}{2} S_{max} L_{Smax} \qquad \text{Eq. 7}$$

Table 1 presents the scour hazard scores. In this case, the selected probability corresponds to the 10-year return period, an intermediate value in the extreme distribution.

2.4.3 Wear hazard

Wear hazard refers to the erosive wear caused by solid particle erosion, the process that occurs on archaeological structures/ artifacts in the seabed exposed to the impact of suspended sediment particles transported by waves. The optimal approach to evaluate this hazard includes estimating the volume of material eroded by a single grain impact (Vi) according to the impact wear equation proposed by Bitter (1963). However, this approach requires specific measurements and the details of the threshold energy required for impact as well as the kinetic energy necessary to erode a unit of volume of material, depending on the status of the different archaeological materials.

This information is not available at the regional or local scale for all the archaeological sites. Therefore, the erosive wear potential ($EWP = log(KE \cdot IR)$) is used as an erosive wear hazard indicator. It is calculated using the kinetic energy ($KE = \frac{1}{2}(M_{sp} U_i^2)$) (where U_i is the grain velocity and M_{sp} the mass of the particle) of the impacting grain considering the direction that maximizes the erosion ($\alpha = 90°$) multiplied by

the impact rate (Thompson et al., 2011) ($IR=C/M_{sp}$ assumed to be proportional to the sediment concentration divided by the mass of the sediment particle.

We can assume $U_i \cong U_b$ considering the low velocity lag between flow and sediment particles in non-concentrated flows (Nian-Sheng, 2004). $M_{sp} = (\frac{4}{3}) \cdot \pi (\frac{D_{50}}{2})^3 (\frac{\rho_s}{\rho})$ is calculated assuming spherical particles, quartz density (ρ_s=2600$kg \cdot m^{-3}$), and seawater density (ρ=1025$kg \cdot m^{-3}$). Sediment concentration was calculated at a reference level of 0.5 m above seabed, assuming a logarithmic profile (van Rijn, 1993).

$$C(z) = C_o \left(\left(h - \frac{z}{z} \right) \left(\frac{a}{h-a} \right) \right)^{\frac{w_s}{ku_*}} \qquad \text{Eq. 8}$$

where h is the water depth accounting for the tidal variability of the sea surface, z is the height above bed, a is the reference level (a=10D_{50}) (Nielsen, 1986), D_{50} being the median particle size; w_s the particle settling velocity, k the von Karman's constant (0.4), and u_* the wave friction velocity.

The reference concentration (C_o) is given from equation Eq. 9, and shield entrainment (θ_s) is given from Eq. 10 as proposed by Zyserman and Fredsøe (1994):

$$C_o = \frac{0.331(\theta_s - 0.045)^{1.75}}{1 + \frac{0.331}{0.46}(\theta_s - 0.045)^{1.75}} \qquad \text{Eq. 9}$$

$$\theta_s = \frac{f_w U_b}{2g\left(\left(\frac{\rho_s}{\rho} \right) - 1 \right)} \qquad \text{Eq. 10}$$

and the critical shield parameter for the initiation of motion is given by the expression proposed by Soulsby (1997):

$$\theta_{cr} = \frac{0.3}{1 + 1.2D_*} + 0.055 \left(1 - exp \left(-0.02D_* \right) \right) \qquad \text{Eq. 11}$$

where D_* is the dimensionless grain diameter:

$$D_* = D_{50} \left[\frac{g\left(\left(\frac{\rho_s}{\rho} \right) - 1 \right)}{\vartheta^2} \right]^{1/3} \qquad \text{Eq. 12}$$

f_w is the wave friction factor for oscillatory flow assuming the sheet flow estimated as follows (van Rijn, 1993):

$$f = \begin{cases} exp\left(-6 + 5.2\left(\frac{A_w}{K_s} \right)^{-0.19} \right) & \text{rough} \quad \text{oscillatory} \quad \text{flow} \quad (Re \geq 1e6) \\ 0.09(U_b A_w/\vartheta)^{-0.2} & \text{smooth} \quad \text{oscillatory} \quad \text{flow} \quad (1.5e5 \leq Re < 1e6) \\ 2(U_b A_w/\vartheta)^{-0.5} & \text{laminar} \quad \text{oscillatory} \quad \text{flow} \quad (Re \leq 1.5e5) \end{cases}$$

$$\text{Eq. 13}$$

$A_w = \frac{Tp}{2\pi} U_b$ is the peak orbital excursion, Tp is the peak wave period, U_b is the undisturbed near-bed orbital velocity, ϑ is the kinematic viscosity (1.075e-6 m^{2}s^{-1}), K_s=2.5D_{50} is the bed roughness (Soulsby, 1997), and $Re=U_b A_w/\vartheta$ is the Reynolds number.

The settling velocity w_s is calculated in accordance with the equation proposed by Soulsby (1997):

$$w_s = \frac{\vartheta}{D_{50}} \left[(10.36^2 + 1.049D_*^3)^{0.5} - 10.36 \right] \qquad \text{Eq. 14}$$

The friction velocity is estimated in accordance with the equation proposed by van Rijn (1993):

$$u_* = \sqrt{\frac{1}{4} \rho f_w U_b^2 / \rho} \qquad \text{Eq. 15}$$

The suspended sediment concentration is calculated for those sea states where the shield number exceeds the critical value ($\theta_s > \theta_{cr}$), and friction velocity is larger than settling velocity ($u_* > w_s$). If any of these conditions is not met, the suspended sediment concentration is assumed to be zero.

Table 1 presents the scores of the erosive wear hazard. In this case, the indicator is based on a high probability event corresponding to a 1-year return period. This high frequency value in the extreme distribution was selected to account for the continuous effect of erosive wear to damage UCH materials rather than the occasional (longer return periods) erosive wear effect that takes place for a limited time in an extreme event.

2.5 Vulnerability assessment

According to the 2009 UNISDR terminology, vulnerability is defined in terms of the *conditions determined by physical, social, economic and environmental factors or processes which increase the susceptibility of an individual, a community, assets, or systems to the impacts of hazards*. In this paper, vulnerability of UCH assets is determined by the characteristics of the archaeological material that prevails in the UCH site (metal, stone, wood, ceramic, and glass) and its tendency to be affected by a certain hazard and the environmental characteristics that increase the susceptibility of the UCH assets to be impacted by a hazard. The vulnerability index for the prevalent materials was established according to the specificity of the UCH site types in the study area and the main characteristics of the archaeological material. Thus, the vulnerability of metallic materials is defined in compliance with the specific properties of gray iron, the most frequent metallic material in the archaeological database of the case study. The ceramic vulnerability was established according to the properties of coarse ware, the type of archaeological artifact most represented in the ADB.

The vulnerability index related to the materials (sm_{vm}^i) is sensitive to the hazard considered. It is therefore defined in conformity with the specific properties of each material to cope with a certain hazard—for instance, stone materials (marble in our ADB) may be more vulnerable to erosive wear hazard than metallic (gray iron) ones, as they stand lower in the Brinell hardness scale or the equivalent hardness scale. However, marble is less vulnerable than gray iron to the impact of the decontextualization hazard based on the higher density

property used to define the propensity of materials to be transported by waves.

The vulnerability index related to the materials ranges from 1 to 5 after assigning a score (1 to 5) to the types of materials (metal, stone, wood, ceramic, and glass). The vulnerability assigned by materials and hazards is summarized in Table 2. It includes the categories and types of materials as well as the properties selected to assign the vulnerability.

Regarding the decontextualization hazard, we did not have real data of the objects in each site. We decided to establish the rank based on the density of the main materials that can be found in the sites. The values in Table 2 are commercial, except in the case of ceramics, and obtained from Vila Socias et al. (2007).

With respect to the erosive wear hazard, Table 2 shows the hardness values of the main types of materials located in the sites on the Brinell scale (Vander Voort, 2000). In the case of stone and wood, the value is established by comparison with another material capable of scratching it. Coarse ware is scratched with steel, which has a Brinell hardness number (BHN) of 125, and oak is scratched with copper, which has a BHN of 35.

In the case of scour hazard, Table 2 ranks the material according to its sensitivity of the aerobic biological communities. The scour processes facilitate the increase of dissolved oxygen transforming the anoxic condition of the sediment into well-oxygenated waters. The aerobic biological communities living in this environment produce the deterioration of the different materials depending on their nature (Pearson, 1987), for example, in the waters of the Bay of Cadiz, wood is badly affected by mollusks of the genus *Teredo*.

Moreover, vulnerability was defined accounting for the environmental factors (seabed slope s_{vss}^i and seabed typology s_{vst}^i), which increase or decrease the susceptibility of the UCH sites to the impacts of each assessed hazard. In this case, the vulnerability index related to the environmental factors was considered constant for all the hazards. According to expert judgment, the higher values of vulnerability level (5) were established for those conditions that significantly amplify the vulnerability, the lower value (1) was established for those conditions that significantly decrease the vulnerability, and a neutral value of 3 was established for those conditions that do not modify the vulnerability. Following this approach, the seabed slope increased the vertical and horizontal velocities and the turbulence because of the modification of waves and current velocity fields. These amplifications cannot be addressed properly with the resolution and processes parametrized in commonly used wave propagation models for coastal applications. They could lead to greater susceptibility of the UCH sites located at a sloped seabed to the impact of the decontextualization, erosive wear, and scour hazards. Therefore, a sloped seabed (>10%) was scored as high vulnerability class (s_{vss}^i=5) and a gentle sloped seabed as medium vulnerability class (s_{vss}^i=3). The second environmental factor considered is the type of seabed. In this paper, two categories, rocky and non-consolidated seabed,

were established in accordance with the seabed characteristics in the case study. However, they can be adapted to other categories (salt marsh vegetation, seagrass meadows, *etc.*). In this case, the UCH sites lying on a rocky seabed were scored as low vulnerability class (s_{vst}^i=1) and those on a non-consolidated one as medium vulnerability class (s_{vst}^i=3). Although the rocky seabed may house sand patches, the limited quantity of sediment potentially reduces the scour, and erosive wear is limited in comparison with the non-consolidated seabed. The decontextualization hazard is reduced because the irregularities in a rocky seabed may protect the archaeological objects hampering scattering by wave action. Table 3 lists the vulnerability scores according to the slope and the type of seabed.

The final vulnerability index S_V^i was calculated as the geometric mean of all the vulnerability indicators, the material-related vulnerability index (sm_{vm}^i) established from the ADB, and the environmental vulnerability indicator (seabed slope index (s_{vss}^i) and seabed type index (s_{vss}^i). These values were stablished from the DEM dataset and the seabed type dataset. The final value of S_V^i may take values from 1, indicating low-vulnerability class, to 5, for the very-high-vulnerability class.

$$S_V^i = \left[sm_{vm}^i \cdot s_{vss}^i \cdot s_{vst}^i \right]^{1/3} \qquad \text{Eq. 16}$$

2.6 Validation of the UCH risk assessment methodology

The *Fougueux* and *Bucentaure* sites were monitored, and metallic archaeological artifacts from each site were analyzed using archaeometric techniques to evaluate their degree of stability (Bethencourt et al., 2018). The result was used to validate the method for UCH risk assessment presented in this paper, focusing on erosive wear and scour hazards. Unfortunately, there are no data available to evaluate the decontextualization hazard in the study area.

At both sites, several cannons and anchors were selected as targets to establish their current conservation condition and to assess their prospects for *in situ* conservation. First, partial de-concretion was carried out, which allowed performing *in situ* measurements of the pH and corrosion potential of the iron object, E_{corr} [see Bethencourt et al. (2018) for further details]. The conservation status of the cannons was assessed by

TABLE 3 Vulnerability scores by environmental factors in underwater cultural heritage sites.

Slope, β (%)	Vulnerability score	Bed type	Vulnerability score
β< 10	3	Rock	1
β ≥ 10	5	Not consolidated	3

measuring the thickness of the surface corrosion layer. Then, the mean corrosion rate of the archaeological object was estimated by dividing the surface corrosion layer by the number of years since wrecking.

The spatial pattern of the corrosion rates measured in the cannons of the *Fougueux* site was analyzed with regard to the seabed type and slope in order to evaluate the vulnerability index related to environmental factors. The method to estimate the erosive wear risk was also validated by comparing the corrosion rates calculated from *in situ* measurement at both sites as a proxy of the erosive wear at the sites.

The accretion–erosion model derived by subtracting different DEM from time lapsed bathymetric surveys conducted in the *Fougueux* and *Bucentaure* sites [see Fernández-Montblanc et al. (2016) and Bethencourt et al. (2018) for further details] was used to evaluate the UCH risk assessment for the scour hazard.

3 Results

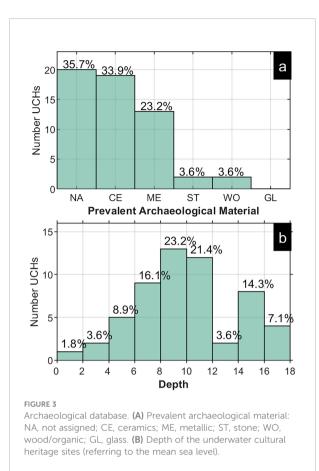## 3.1 Archaeological database

The ADB incorporated a total of 56 UCH sites located at the outer Bay of Cadiz. Regarding the archaeological material, ceramic (34%) and metallic (23%) materials are the most commonly prevalent materials in the UCH sites where this information is available. In the ADB, UCH sites are rarely composed of prevalent materials such as wood and stone (~4%). The ADB included 36% of the UCH sites without information relative to the archaeological material corresponding to the modern period (Figure 3A). For that period, metal was the most common material in the rest of the UCH sites included in the database when that information was available in the bibliographic references. Therefore, we assigned the metallic material as prevalent in those UCH sites lacking information relative to the material composition. Most of the sites (~47%) range from 8 to 12 m in depth, and few of them (5%) are in very shallow water (<4 m) (Figure 3B).

The bibliographic sources used to build the ADB include the main materials present in these sites. We divided them into five categories, each represented by the most common material, namely: metallic (gray iron), stone (marble), glass (glass), ceramics (coarse ware), and wood/organic (oak).

3.2 Hazard assessment in the Bay of Cadiz

3.2.1 Decontextualization hazard

Figure 4A shows the distribution of the maximum critical size of an object that could be moved due to wave action in a 10-year return period (RT10). Overall, the area is characterized by an average value of 0.12 m. Values larger than 0.15 m of critical size were observed in 25% of the outer bay, mostly in shallower

FIGURE 3
Archaeological database. **(A)** Prevalent archaeological material: NA, not assigned; CE, ceramics; ME, metallic; ST, stone; WO, wood/organic; GL, glass. **(B)** Depth of the underwater cultural heritage sites (referring to the mean sea level).
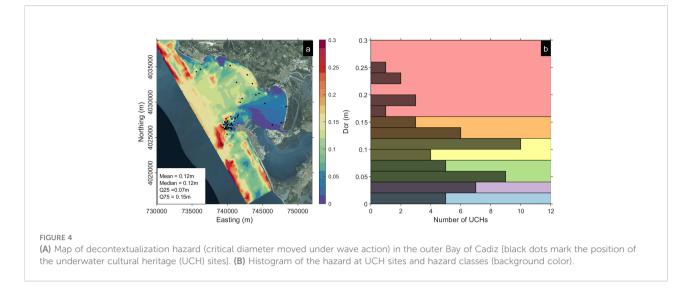
regions. Figure 4B relates the number of UCH sites located in areas with the different classes of hazard. Seven UCH sites are located in very-high-hazard areas (Dcr ≥ 0.16 m) and nine in high-hazard areas (0.12 ≤ Dcr< 0.16).

3.2.2 Scour hazard

The spatial pattern of scour hazard represented by the potential scour volume corresponding to RT10 is presented in Figure 5A. A potential scour volume of 0.32 m^3 is observed in most of the area, while values >0.5 m^3 can be observed in the north, central, and southern coastal areas. Most of the UCH sites (~38%) show SC hazard values ranging from 0.3 to 0.4 m^3. Only one UCH site is located in an area with a very high hazard category (>0.7 m^3), while four UCH sites (0.5–0.6 m^3) are in areas categorized as high-hazard areas (Figure 5B).

3.2.3 Erosive wear hazard

The erosive wear hazard ranges from -16 to -12 (Figure 6A). Most of the area is characterized by -13.5. The higher erosion potential (< -12.5) was observed in the mouth of the bay and in the southern areas. These areas combine higher wave bed shear stress and orbital velocity with finer sediment that can be easily resuspended. Most of the sites (~70%) in the central area are located in medium–high hazard areas, whereas only one UCH site was affected by high EW hazard (Figure 6B).

FIGURE 4
(A) Map of decontextualization hazard (critical diameter moved under wave action) in the outer Bay of Cadiz [black dots mark the position of the underwater cultural heritage (UCH) sites]. **(B)** Histogram of the hazard at UCH sites and hazard classes (background color).

3.3 UCH risk assessment in the Bay of Cadiz
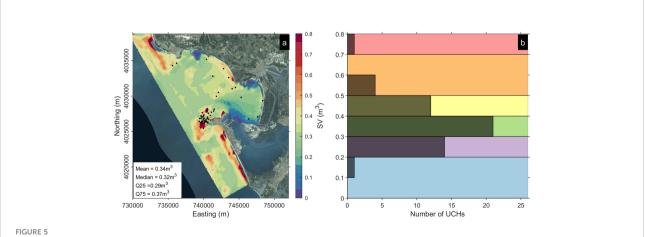
3.3.1 Decontextualization risk

The calculated $UCHR_{DE}$ risk indexes are distributed around the median value of 2.5 (Figures 7A, B). The UCH sites with higher $UCHR_{DE}$ values (>3) are located in the southern area of the mouth of the Bay of Cadiz (Figure 8A), where six UCH sites exceeding the threshold of 3.2 are located (Figure 7B). Metallic materials are prevalent in five of them, and only one is a ceramic material site showing a higher $UCHR_{DE}$ value (3.6). The UCHs composed of wood—therefore with a higher vulnerability index related to the prevalent material—are located in a low-energy area at the sandy coast of the inner bay characterized by low-wave orbital velocities.
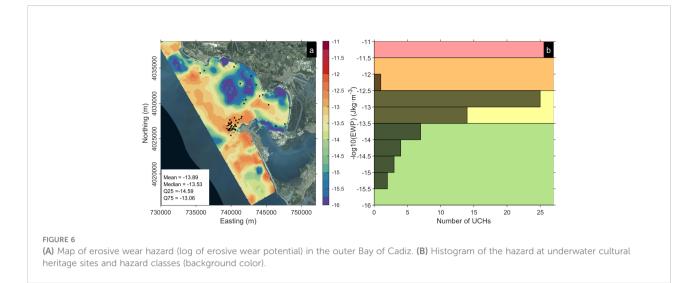
3.3.2 Scour risk

The $UCHR_{SC}$ index oscillates between low–medium and medium–high values (1.5-2.5) in most of the UCH sites registered in the ADB (Figures 8A, B). A total of four UCH sites were identified as high-risk sites, all of them in the southern side of the mouth of the Bay of Cadiz (Figure 8A). Three of these UCH sites correspond to sites where metallic materials prevail, including the site with a higher $UCHR_{SC}$ (3.94). Only one site is composed of ceramic material ($UCHR_{SC}$ =3.87). The risk index in wooden UCH sites increases compared with the decontextualization hazard, with maximum values of 2.7.

3.3.3 Erosive wear risk

The risk imposed by the erosive wear hazard is depicted in Figure 9. The $UCHWR_{WE}$ index shows the lower spread (Sd = 0.35)

FIGURE 5
(A) Map of scour hazard (scour volume) in the outer Bay of Cadiz. **(B)** Histogram of the hazard at underwater cultural heritage sites and hazard classes (background color).

FIGURE 6
(A) Map of erosive wear hazard (log of erosive wear potential) in the outer Bay of Cadiz. **(B)** Histogram of the hazard at underwater cultural heritage sites and hazard classes (background color).
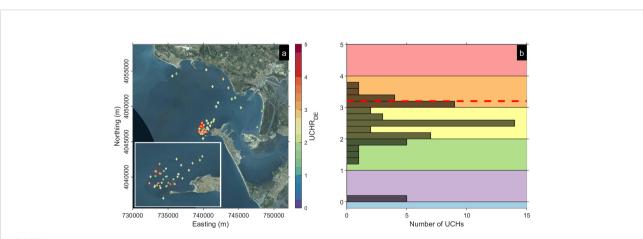
among the hazards analyzed. The most frequent categories of erosive wear risk for the UCH sites in the Bay of Cadiz are medium–high and high (Figures 9A, B). However, only two sites exceed $UCHR_{WE}$ >3.2. As in the previous cases, these sites are located in the area with a higher concentration of UCH sites. Those UCH sites include one site composed of metallic artifacts ($UCHR_{WE}$ = 3.24) and another site where ceramic is the prevailing material ($UCHR_{WE}$ = 3.27).

3.4 Validation of the UCH risk assessment methodology for erosive wear and scour hazards
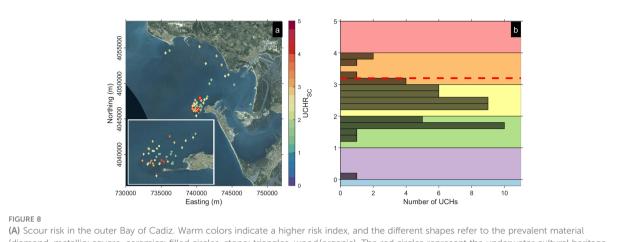
The qualitative assessment of the vulnerability index related to the environmental factors in comparison with the estimated

corrosion rates (CR) of cannons at the *Fougueux* site indicates a good correlation between the higher values of corrosion rates in metallic artefacts and the seabed type and slope. Higher values of CR are associated to cannons located in sandy seabeds and slopes >10% (Figure 10). The statistical significance of the differences in the averages of CR of each group of cannons according to the environmental factor was evaluated through a *t*-test. A comparison between cannons located on a sandy bottom (0.20 mm·year^{-1}) and on a rocky bottom (0.22 mm·year^{-1}) indicates significant differences (*p*-value = 0.03) at 0.05% significance level. No significant differences were found between gentle slope seabeds (<10%) (0.21 mm·year^{-1}) and sloped seabeds (0.24 mm·year^{-1}), although only one cannon was on a sloped seabed, thus reducing the test validity.

Regarding the risk assessment, good agreement was observed between CR, the proxy used to estimate the erosive

FIGURE 7
(A) Decontextualization risk in the outer Bay of Cadiz. Warm colors indicate a higher risk index, and the different shapes refer to the prevalent material (diamond, metallic; square, ceramics; filled circles, stone; triangles, wood/organic). The red circles represent the underwater cultural heritage (UCH) sites where $UCHR_DE$ >3.2. **(B)** Histogram of the decontextualization risk index. The red dashed line shows the threshold (3.2) used to identify UCH sites at risk.

FIGURE 8
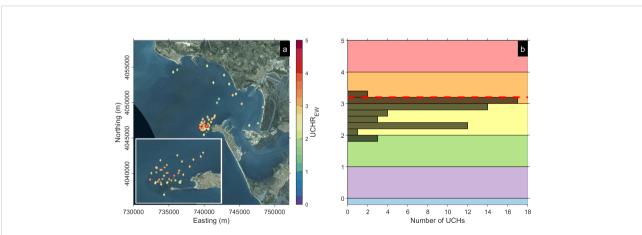**(A)** Scour risk in the outer Bay of Cadiz. Warm colors indicate a higher risk index, and the different shapes refer to the prevalent material (diamond, metallic; square, ceramics; filled circles, stone; triangles, wood/organic). The red circles represent the underwater cultural heritage (UCH) sites where $UCHR_{SC}$ >3.2. **(B)** Histogram of the scour risk index. The red dashed line shows the threshold (3.2) used to identify UCH sites at risk.

wear impact, and the erosive wear risk index calculated at the *Fougueux* and *Bucentaure* sites (Table 4). The averages of the cannons' CR were 0.11 mm·year⁻¹ at the *Bucentaure* site and 0.22 mm·year⁻¹ at the *Fougueux* site. The difference is statistically significant according to the *t*-test (*p*-value = 2e-9). These values of corrosion rates correspond to 0 and 3.27 erosive wear risk index, indicating a large difference that marks the *Fougueux* site over the threshold to mark high-risk sites. No re-suspension was observed for the *Bucentaure* site that could lead to erosive wear potential (EWP) (S_H=0), whereas the EWP for RT10 was 9.5e-13 (S_H=4) at the *Fougueux* site. The vulnerability score was similar at both sites (S_V = 2.67), which is the result of gentle slopes (s_{vss}=3) and sandy seabed as the dominant seabed types in the
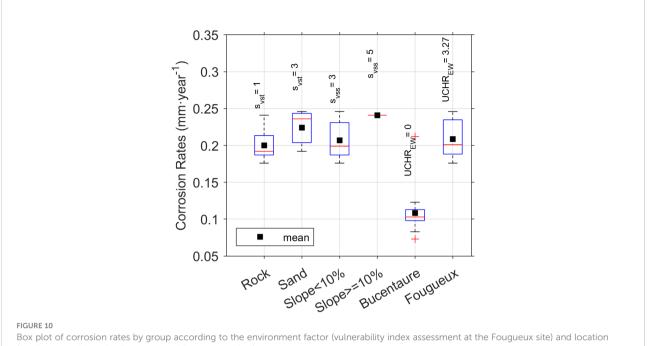
sites (s_{vst}=3) and gray iron as the prevalent material (sm_{vm}=2). Although the corrosion rates provide integrated information of all degradation processes related to the marine conditions, erosive wear was recognized as the key process after completing a meticulous monitoring program in the sites[4].

With respect to the scour risk assessment evaluation, the methodology highlights both sites as UCH sites at risk. The scour risk index presents higher values at the *Fougueux* site (3.65), whereas at the *Bucentaure* site (3.27) it slightly exceeds the threshold (3.2). This classification reflects the observations of the drastic morpho-dynamic changes (Smax = 0.7 m) at the *Fougueux* site compared with those observed at the *Bucentaure* site (Smax = 0.3 m) (Table 4).

FIGURE 9
(A) Erosive wear risk in the outer Bay of Cadiz. Warm colors indicate a higher risk index, and the different shapes refer to the prevalent material (diamond, metallic; square, ceramics; filled circles, stone; triangles, wood/organic). The red circles represent underwater cultural heritage (UCH) where $UCHR_{SC}$ >3.2. **(B)** Histogram of the erosive wear risk index. The red dashed line shows the threshold (3.2) used to identify UCH sites at risk.

FIGURE 10
Box plot of corrosion rates by group according to the environment factor (vulnerability index assessment at the Fougueux site) and location (erosive wear risk at the Fougueux and Bucentaure sites).

4 Discussion

As a part of maritime cultural heritage, UCH constitutes a non-renewable cultural resource that must be preserved. UCH is only related to tangible assets and resources, while maritime heritage includes intangible assets (Kyvelou et al. 2022). Hence, UCH is a finite resource affected by natural threats (*e.g.,* shipworms, microbiological decay, erosion, natural hazards) or anthropogenic pressures (*e.g.,* pollution, dredging, bottom trawling using a dragnet, pillage). Among the natural threats, wave-induced hazards are a key player for the preservation of UCH in shallow water. This paper adapts the CRAFT1 methodology for coastal risk assessment (Armaroli and Duo, 2018; Ferreira et al., 2018) and presents a new methodology for UCH risk assessment associated to wave-induced hazards. This methodology can be adjusted and expanded to include other natural or anthropogenic-induced hazards. There are some

studies that focus on other specific hazards such us ship anchoring damage (Aps et al., 2020) or damage caused by bottom trawling to ancient shipwreck sites (Brennan et al., 2016). To the best of our knowledge, no similar methodological developments have been applied to UCH risk assessment to evaluate wave impact. This risk assessment method includes the quantification of the probability of the hazard and the vulnerability of UCH sites at risk in a systematic and transparent manner that facilitates the adoption of the methodology for UCH managers as well as the adaptation to their necessities.

Identifying UCH sites at risk is the first step in UCH protection and preservation. It requires a concentrated effort and allows optimizing protection measures at specific sites. Additionally, risk assessment enables identifying the threatened UCH sites, which is key to include UCH in maritime spatial planning (Kyvelou et al. 2022; Papageorgiou,

TABLE 4 Qualitative validation of erosive wear risk (average corrosion rates $\pm$ standard deviation) and scour risk (maximum scour) measured in the sites.

Site	RT1 E erosive wear potential (J/m^3)	RT10-scouring volume (m^3)	S_H	S_V	Erosive wear risk index	Scour risk index	Corrosion rates (mm·year^{-1})	Smax (m)
Erosive wear								
Bucentaure	0		0	2.67	0		0.11 ± 0.04	
Fougueux	9.5e^{-13}		4	2.67	3.27		0.21 ± 0.03	
Scour								
Bucentaure		0.62	4	2.67		3.27		0.3
Fougueux		1.09	5	2.67		3.65		0.7

2018). This is particularly important in the era of a sustainable blue economy where UCH, beyond its undeniable social and cultural value, can be considered a resource with uses of socio-economic relevance (Papageorgiou, 2019).

The proposed methodology is based on indicators that follow the principles of acceptability, reliability, simplicity of application, and low data requirements (Alexandrakis and Poulos, 2014). The acceptability of this methodology relies on the transparency of the methods for hazard and vulnerability computation as well as on the flexibility to be adapted for a specific coastal environment and the completeness of the ADB—for instance, the protective role of some ecosystems diminishing wave energy such as seagrass meadows (Infantes et al., 2012) can be incorporated by defining new categories in the seabed vulnerability index. Similarly, the ADB could be completed by incorporating other archaeological materials. The expertise and know-how of the managers and decision-makers could also be considered as well as changing the ranks of the hazards and vulnerability or the chosen probabilities (i.e., RT1 for erosive wear or RT10 for scour and decontextualization hazards).

The methodology, built upon simple empirical models for the hazard computation, reduces the uncertainties associated to the many parameters appearing in more complex process-based models. It increases the reliability of the hazard computation methods considering the target of hazard intercomparison between different UCH sites. The reliability of the methodology including hazard and vulnerability components was evaluated for scour and erosive wear showing a good correlation with in situ measurements of scour and corrosion rates (used as a proxy of erosive wear). It is difficult to validate the UCH risk assessment for the decontextualization hazard given the lack of field measurements to quantify UCH decontextualization. The validation of UCH risk assessment should be expanded to different coastal environments covering various wave energy conditions and sediment characteristics and UCH sites containing different archaeological materials. The additional advantages of the method are the simplicity of the application and the low amount and availability of the required data. These advantages are related to the use of a simple empirical model and to the fact that the environmental information about depth and seabed type is readily available from nautical charts. The use of process-based models, i.e., hydro-morphodynamic models, would be more accurate from the physical–chemical point of view, but there would be more uncertainties, and the simplicity of the interpretation of results would be reduced. They would also require a large amount of high-quality data for proper regional applications.

4.1 Limitations and challenges for UCH risk assessment

The use of a simple empirical model for hazard quantification overlooks several processes of major relevance for the analyzed
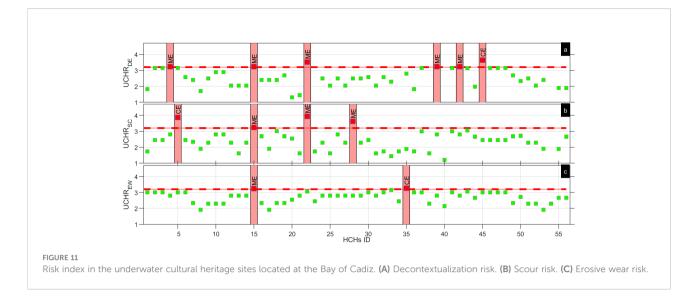
hazards, such as flow speed and turbulence enhancement, because of flow–structure interaction (Fernández-Montblanc et al., 2018; Quinn and Smyth, 2018). The inclusion of these processes would request high-resolution bathymetry (<1 m) and an enormous computational effort necessary for computational fluid dynamics. These limitations can be overcome at a later stage when a new risk assessment including these processes is targeted at UCH sites at high risk in order to provide accurate solutions to design protection measures. Other secondary processes such as the enhancement of bed shear stress due to the effect of wave–current interaction (Soulsby and Clarke, 2005) and wave–tide interaction (Kagan et al., 2001), accounting for the influence of bottom mobility (Kagan et al., 2005), sediment load stratification (Kagan et al., 2003), or the modification sediment concentration by the bed forms (Nielsen, 1986), can be incorporated using empirical and theoretical models.

In this paper, risk assessment was conducted for each hazard separately. Nevertheless, Figure 11 illustrates the concurrency of the three analyzed hazards in a single UCH site (Id15) and scour and decontextualization hazard concurrency (Id17). A multi-hazard analysis should be incorporated to evaluate if the hazardous events occur simultaneously in a cascading or cumulative manner over time (UNISDR, 2017)—for example, scour in sites Id15 and Id17 would facilitate the decontextualization of buried archaeological objects in those sites.

Regarding the vulnerability quantification, the limitations are linked to an ADB built upon bibliographic research. Underwater ADBs are very scarce, incomplete, or not publicly available to prevent illicit actions (Papageorgiou, 2019). These databases would allow identifying patterns affecting UCH and taking actions, which is often hampered by the lack of accessible data (Andreou et al., 2022). A more complete ADB in terms of UCH site characterization would allow the improvement of vulnerability quantification, i.e., including chronology or conservation status as an additional vulnerability index. Additionally, it would allow expanding the analysis from a single prevalent material to all the materials that constitute the UCH site, thus providing a more complete UCH risk assessment.

Exposure is considered equal for all the UCH sites included in the ADB because of a lack of information. Quantifying exposure should be addressed through the valuation of UCH. The valuation of UCH includes the cultural capital or non-extractive value and the extractive or market-associated value as well as cultural tourism and recreational activities (Claesson, 2011). This information is key to know if an UCH site is worth being protected. Including this information could change the nine UCH sites at risk identified in the Bay of Cadiz.

Finally, the risk index definition should take the objectives and expertise of the stakeholders involved in UCH management into account by means of a participative process. It has been demonstrated in other disciplines that the involvement of stakeholders in risk assessment for the definition of vulnerability, hazard type, and risk thresholds allows gathering

FIGURE 11
Risk index in the underwater cultural heritage sites located at the Bay of Cadiz. **(A)** Decontextualization risk. **(B)** Scour risk. **(C)** Erosive wear risk.

useful information to improve the indicators and to increase confidence in the risk assessment (Meadow et al., 2015; Viavattene et al., 2018).

5 Concluding remark

This paper presents a novel UCH risk assessment methodology to quantitatively assess the impact of wave-induced hazards on UCH in the coastal environment and to give precedence to the UCH sites at high risk. The risk assessment was performed for decontextualization, scour and erosive wear, and major natural hazards threatening the preservation of UCH in shallow water areas.

The methodology was validated at the *Bucentaure* and *Fougueux* sites through a comparative analysis including *in situ* measurements. The validation showed a good correlation between the risk index and the *in situ* measurements of scour and corrosion rates (used as a proxy of erosive wear). The methodology was tested in the Bay of Cadiz using an ADB containing 56 UCH sites, with metallic and ceramic materials being prevalent in most of them. The sites are seated at a depth ranging from 6 to 12 m. The methodology allowed identifying the UCH sites at high risk in the Bay of Cadiz: six are at risk of decontextualization, four are in peril of scour, and two are at risk of erosive wear. Moreover, the UCH risk assessment revealed the concurrency of at least two hazards in two of the UCH sites at high risk.

Even though the methodology has only been validated in a specific coastal environment, showing limitations related to the completeness of the ADB, it is a steppingstone towards a decision support system that will give priority to research, prospection, management, and protection measures in the UCH sites analyzed to ensure their preservation in the context of climate change in the era of a sustainable blue economy.

Data availability statement

The datasets presented in this article are not readily available, as raw data will be available on request with the exception of the archaeological data-base to ensure underwater cultural heritage preservation.Requests to access the datasets should be directed to tomas.fernandez@uca.es.

Author contributions

TF-M: conceptualization, methods, investigation, formal analysis, visualization, writing the original draft, writing, review and editing, management and coordination of the project. MB: methods, writing, review and editing, management and coordination of the project. AI: conceptualization, writing, review and editing. All authors contributed to the article and approved the submitted version.

Funding

Conflict of interest

The authors declare that the research was conducted in the absence of any commercial or financial relationships that could be construed as a potential conflict of interest.

Publisher's note

All claims expressed in this article are solely those of the authors and do not necessarily represent those of their affiliated organizations, or those of the publisher, the editors and the reviewers. Any product that may be evaluated in this article, or claim that may be made by its manufacturer, is not guaranteed or endorsed by the publisher.

References

Alexandrakis, G., and Poulos, S. E. (2014). An holistic approach to beach erosion vulnerability assessment *Sci. Rep.* 4, 6078. doi: 10.1038/srep06078

Alzaga García, M., Márquez Carmona, L., Rodríguez Mariscal, N., Martí Solano, J., Higueras-Milena Castellano, A., Gallardo Abárzuza, M., et al. (2022). *Shipwrecks of the Iberian tradition in the Bay of Cadiz (Andalucía, Spain) BT - heritage and the Sea: Volume 2: Maritime history and archaeology of the global Iberian world (15th–18th centuries)*. Eds. A. Crespo Solana, F. Castro and N. Nayling (Cham: Springer International Publishing), 145–167. doi: 10.1007/978-3-030-86464-4_6

Andreou, G. M., Nikolaus, J., Westley, K., el Safadi, C., Blue, L., Smith, A., et al. (2022). Big data in maritime archaeology: Challenges and prospects from the middle East and north Africa. *J. F. Archaeol.* 47, 131–148. doi: 10.1080/00934690.2022.2028082

Angelini, E., Grassini, S., Tusa, S.A. B. T.-C. and C. @ of C. H. M. A. Adriaens (2013). "12 - underwater corrosion of metallic heritage artefacts," in *European Federation of corrosion (EFC) series*. Eds. P. Dillmann, D. Watkinson and E. Angelini (Oxford: Woodhead Publishing), 236–259. doi: 10.1533/9781782421573.3.236

Aps, R., Lees, L., Herkül, K., Roio, M., and Tõnismaa, O. (2020). Towards STAMP approach based protection of underwater cultural heritage. *Proc. Int. Semin. Saf. Secur. Auton. Vessel. Eur. STAMP Work. Conf.* 2019, 169–178. doi: 10.2478/9788395669606-014

Armaroli, C., and Duo, E. (2018). Validation of the coastal storm risk assessment framework along the Emilia-romagna coast. *Coast. Eng.* 134, 159–167. doi: 10.1016/J.COASTALENG.2017.08.014

Bethencourt, M., Fernández-Montblanc, T., Izquierdo, A., González-Duarte, M. M., and Muñoz-Mas, C. (2018). Study of the influence of physical, chemical and biological conditions that influence the deterioration and protection of underwater cultural heritage. *Sci. Total Environ.*, 613–614, 98–114. doi: 10.1016/j.scitotenv.2017.09.007

Bitter, J. G. A. (1963). A study of erosion phenomena part I. *Wear* 6, 5–21. doi: 10.1016/0043-1648(63)90003-6

Björdal, C. G., Daniel, G., and Nilsson, T. (2000). Depth of burial, an important factor in controlling bacterial decay of waterlogged archaeological poles. *Int. Biodeterior. Biodegrad.* 45, 15–26. doi: 10.1016/S0964-8305(00)00035-4

Björdal, C. G., and Nilsson, T. (2008). Reburial of shipwrecks in marine sediments: a long-term study on wood degradation. *J. Archaeol. Sci.* 35, 862–872. doi: 10.1016/j.jas.2007.06.005

Blott, S. J., and Pye, K. (2001). GRADISTAT: a grain size distribution and statistics package for the analysis of unconsolidated sediments. *Earth Surf. Process. Landforms* 26, 1237–1248. doi: 10.1002/esp.261

Booij, N., Ris, R. C., and Holthuijsen, L. H. (1999). A third-generation wave model for coastal regions 1. model description and validation. *J. Geophys. Res. Ocean.* 104, 7649–7666. doi: 10.1029/98JC02622

Brennan, M. L., Davis, D., Ballard, R. D., Trembanis, A. C., Vaughn, J. I., Krumholz, J. S., et al. (2016). Quantification of bottom trawl fishing damage to ancient shipwreck sites. *Mar. Geol.* 371, 82–88. doi: 10.1016/j.margeo.2015.11.001

Cámara, B., de Buergo, M. Á., Bethencourt, M., Fernández-Montblanc, T., La Russa, M. F., Ricca, M., et al. (2017). Biodeterioration of marble in an underwater environment. *Sci. Total Environ.* 609, 109–122. doi: 10.1016/j.scitotenv.2017.07.103

Camus, P., Mendez, F. J., Medina, R., and Cofiño, A. S. (2011). Analysis of clustering and selection algorithms for the study of multivariate wave climate. *Coast. Eng.* 58, 453–462. doi: 10.1016/j.coastaleng.2011.02.003

Claesson, S. (2011). The value and valuation of maritime cultural heritage. *Int. J. Cult. Prop.* 18, 61–80. doi: 10.1017/S0940739111000051

Diaz-Hernandez, G., Rodríguez Fernández, B., Romano-Moreno, E., and XXXL. Lara, J. (2021). An improved model for fast and reliable harbour wave agitation assessment. *Coast. Eng.* 170, 104011. doi: 10.1016/J.COASTALENG.2021.104011

Fernández-Montblanc, T., Izquierdo, A., Quinn, R., and Bethencourt, M. (2018). Waves and wrecks: A computational fluid dynamic study in an underwater archaeological site. *Ocean Eng.* 163, 232–250. doi: 10.1016/j.oceaneng.2018.05.062

Fernández-Montblanc, T., Quinn, R., Izquierdo, A., and Bethencourt, M. (2016). Evolution of a shallow water wave-dominated shipwreck site: Fougueux, (1805), Gulf of Cadiz. *Geoarchaeology* 31, 487–505. doi: 10.1002/gea.21565

Ferreira, O., Viavattene, C., Jiménez, J. A., Bolle, A., das Neves, L., Plomaritis, T. A., et al. (2018). Storm-induced risk assessment: Evaluation of two tools at the regional and hotspot scale. *Coast. Eng.* 134, 241–253. doi: 10.1016/J.COASTALENG.2017.10.005

Field, C., and Barros, V. (2014) *Climate change 2014–impacts, adaptation and vulnerability: Regional aspects*. Available at: https://books.google.com/books?hl=es&lr=&id=aJ-TBQAAQBAJ&oi=fnd&pg=PA1142&ots=v2QuHId8HG&sig=aL_w43yxj2tjPCqJRXSKatyJt24 (Accessed May 7, 2022).

García Rivera, C., and Alonso Villalobos, C. (2005) *(16) (PDF) Los naufragios de Trafalgar*. Sevilla: Junta de Andalucía, Consejería de Cultura.

Garrity, N. J., Battalio, R., Hawkes, P. J., and Roupe, D. (2007). Evaluation of event and response approaches to estimate the 100-year coastal flood for pacificcoast sheltered waters. *Coast. Eng. 2006, World Scientific Publishing Company*, 1651–1663. doi: 10.1142/9789812709554_0140

González-Duarte, M. M., Fernández-Montblanc, T., Bethencourt, M., and Izquierdo, A. (2018). Effects of substrata and environmental conditions on ecological succession on historic shipwrecks. *Estuar. Coast. Shelf Sci.* 200, 301–310. doi: 10.1016/j.ecss.2017.11.014

Gornitz, V. (1990). Vulnerability of the East coast, USA to future sea level rise. *J. Coast. Res.* 9(1), 201–237. Available at: http://www.jstor.org/stable/44868636

Gregory, D. (2020). Characterizing the preservation potential of buried marine archaeological sites. *Herit* 3, 838–857. doi: 10.3390/HERITAGE3030046

Gregory, D., Jensen, P., and Strætkvern, K. (2012). Conservation and *in situ* preservation of wooden shipwrecks from marine environments. *J. Cult. Herit.* 13, S139–S148. doi: 10.1016/j.culher.2012.03.005

Guillemot, E., and Meanteau, L. *Mapa fisiográfico del litoral atlántico de Andalucía: 1/50.000 - publicaciones - junta de andalucía*. Available at: https://www.juntadeandalucia.es/servicios/publicaciones/detalle/48731.html (Accessed July 8, 2022).

Infantes, E., Orfila, A., Simarro, G., Terrados, J., Luhar, M., and Nepf, H. M. (2012). Effect of a seagrass (*Posidonia Oceanica*) meadow on wave propagation. *Mar. Ecol. Prog. Ser.* 456, 63–72. doi: 10.3354/meps09754

Kagan, B. A., Alvarez, O., and Izquierdo, A. (2005). Weak wind-wave/tide interaction over fixed and moveable bottoms: a formulation and some preliminary results. *Cont. Shelf Res.* 25, 753–773. doi: 10.1016/j.csr.2004.09.021

Kagan, B. A., Álvarez, O., Izquierdo, A., Mañanes, R., Tejedor, B., and Tejedor, L. (2003). Weak wave/tide interaction in suspended sediment-stratified flow: a case study. *Estuar. Coast. Shelf Sci.* 56, 989–1000. doi: 10.1016/S0272-7714(02)00306-2

Kagan, B. A., Tejedor, L., Álvarez, O., Izquierdo, A., Tejedor, B., and Mañanes, R. (2001). Weak wave–tide interaction formulation and its application to Cádiz bay. *Cont. Shelf Res.* 21, 697–725. doi: 10.1016/S0278-4343(00)00099-6

Kyvelou, S. S., and Henocque, Y.. (2022). How to incorporate underwater cultural heritage into maritime spatial Planning: guidelines and good practices. *EUROPEAN COMMISSION European Climate, Infrastructure and Environment Executive Agency Unit D.3 – Sustainable Blue Economy*. Luxemburg: Publications Office of the European Union.

Lagostena, L. G. (2009). *Catálogo del Patrimonio Histórico del Parque Metropolitano Los toruños*. Sevilla: Junta de Andalucía.

Lakey, D. C. (1987). *Shipwrecks in the Gulf of Cadiz: a catalog of historically documented wrecks from the fifteenth through the nineteenth centuries, Institute of Nautical Archaeology (U.S.)*. Texas A & M University: United States-Spanish Joint Committee for Cultural and Educational Cooperation.

McNinch, J. E., Wells, J. T., and Trembanis, A. C. (2006). Predicting the fate of artefacts in energetic, shallow marine environments: an approach to site management. *Int. J. Naut. Archaeol.* 35, 290–309. doi: 10.1111/j.1095-9270.2006.00105.x

Meadow, A. M., Ferguson, D. B., Guido, Z., Horangic, A., Owen, G., and Wall, T. (2015). Moving toward the deliberate coproduction of climate science knowledge. *Weather. Clim. Soc* 7, 179–191. doi: 10.1175/WCAS-D-14-00050.1

Mentaschi, L., Vousdoukas, M. I., Voukouvalas, E., Dosio, A., and Feyen, L. (2017). Global changes of extreme coastal wave energy fluxes triggered by intensified teleconnection patterns. *Geophys. Res. Lett.* 44, 2416–2426. doi: 10.1002/2016GL072488

Mentaschi, L., Vousdoukas, M., Voukouvalas, E., Sartini, L., Feyen, L., Besio, G., et al. (2016). The transformed-stationary approach: a generic and simplified methodology for non-stationary extreme value analysis. *Hydrol. Earth Syst. Sci.* 20, 3527–3547. doi: 10.5194/hess-20-3527-2016

Nian-Sheng, C. (2004). Analysis of velocity lag in sediment-laden open channel flows. *J. Hydraul. Eng.* 130, 657–666. doi: 10.1061/(ASCE)0733-9429(2004)130:7 (657)

Nielsen, P. (1986). Suspended sediment concentrations under waves. *Coast. Eng.* 10, 23–31. doi: 10.1016/0378-3839(86)90037-2

Papageorgiou, M. (2018). Underwater cultural heritage facing maritime spatial planning: Legislative and technical issues. *Ocean Coast. Manage.* 165, 195–202. doi: 10.1016/j.ocecoaman.2018.08.032

Papageorgiou, M. (2019). Stakes and challenges for underwater cultural heritage in the era of blue growth and the role of spatial planning: Implications and prospects in Greece. *Herit* 2, 1060–1069. doi: 10.3390/HERITAGE2020069

Pearson, C. (1987). *Conservation of marine archaeological objects* (London; Boston: Butterworths).

Pournou, A. (2018). Assessing the long-term efficacy of geotextiles in preserving archaeological wooden shipwrecks in the marine environment. *J. Marit. Archaeol.* 13, 1–14. doi: 10.1007/S11457-017-9176-9

Quinn, R. (2006). The role of scour in shipwreck site formation processes and the preservation of wreck-associated scour signatures in the sedimentary record - evidence from seabed and sub-surface data. *J. Archaeol. Sci.* 33, 1419–1432. doi: 10.1016/J.JAS.2006.01.011

Quinn, R., and Smyth, T. A. G. (2018). Processes and patterns of flow, erosion, and deposition at shipwreck sites: a computational fluid dynamic simulation. *Archaeol. Anthropol. Sci.* 10, 1429–1442. doi: 10.1007/s12520-017-0468-7

Ruuskanen, A. T., Kraufvelin, P., Alvik, R., Díaz, E. R., Honkonen, J., Kanerva, J., et al. (2015). Benthic conditions around a historic shipwreck: Vrouw maria, (1771)) in the northern Baltic proper. *Cont. Shelf Res.* 98, 1–12. doi: 10.1016/j.csr.2015.02.006

Soulsby, R. (1997). *Dynamics of marine sands* (London: Thomas Telford Publishing). doi: 10.1680/doms.25844

Soulsby, R. L., and Clarke, S. (2005). *Bed shear-stresses under combined waves and currents on smooth and rough beds produced within defra project FD1905 Technical Report*. Wallingford: HR Wallingford.

Spanish Ministry of Agriculture, Food and Environment. (2012). *Data from: Plan de Ecocartografías del litoral Español.*

Sumer, B. M., and Fredsøe, J. (1990). Scour below pipelines in waves. *J. Waterw. Port Coastal Ocean Eng.* 116, 307–323. doi: 10.1061/(ASCE)0733-950X(1990)116:3(307

Sumer, B. M., and Fredsøe, J. (2002). The mechanics of scour in the marine environment. *World Sci Singapore*. doi: 10.1142/4942

Thompson, C. E. L., Ball, S., Thompson, T. J. U., and Gowland, R. (2011). The abrasion of modern and archaeological bones by mobile sediments: the importance of transport modes. *J. Archaeol. Sci.* 38, 784–793. doi: 10.1016/J.JAS.2010.11.001

UNISDR (2017) *National disaster risk assessment words into action guidelines governance system, methodologies, and use of results.* Available at: https://www.unisdr.org/files/52828_nationaldisasterriskassessmentpart1.pdf (Accessed July 4, 2022).

Vander Voort, G. F. (2000). Microindentation hardness testing. *Mech. Test. Eval.* 8, 0. doi: 10.31399/asm.hb.v08.a0003272

van Rijn, L. C. (1993). *Principles of sediment transport in rivers, estuaries and coastal seas*. Amsterdam: Aqua publications

Viavattene, C., Jiménez, J. A., Ferreira, O., Priest, S., Owen, D., and McCall, R. (2018). Selecting coastal hotspots to storm impacts at the regional scale: a coastal risk assessment framework. *Coast. Eng.* 134, 33–47. doi: 10.1016/J.COASTALENG.2017.09.002

Vila Socias, L., Hein, A., Kilikoglou, V., and Buxeda i Garrigós, J. (2007). Disseny amforal i canvi tecnològic al voltant del canvi d'era: L'aportació de l'Anàlisi d'Elements finits. *Empúries* 55, 27–38. Available at: https://raco.cat/index.php/Empuries/article/view/138911

Ward, I. A. K., Larcombe, P., and Veth, P. (1999). A new process-based model for wreck site formation. *J. Archaeol. Sci.* 26, 561–570. doi: 10.1006/JASC.1998.0331

Whitehouse, R. (1998). *Scour at marine structures* (London: Thomas Telford Publishing). doi: 10.1680/sams.26551

Young, D. M., and Testik, F. Y. (2009). Onshore scour characteristics around submerged vertical and semicircular breakwaters. *Coast. Eng.* 56, 868–875. doi: 10.1016/J.COASTALENG.2009.04.003

Zyserman, J. A., and Fredsøe, J. (1994). Data analysis of bed concentration of suspended sediment. *J. Hydraul. Eng.* 120, 1021–1042. doi: 10.1061/(ASCE)0733-9429(1994)120:9(1021